Acta Crystallographica Section D
Biological Crystallography
ISSN 0907-4449

Crystallization and preliminary X-ray diffraction analysis of the catalytic domain of recombinant human phosphodiesterase 3B

Sangita B. Patel,[a] Jeffrey P. Varnerin,[b] Michael R. Tota,[b] Scott D. Edmondson,[a] Emma R. Parmee,[a] Joseph W. Becker[a] and Giovanna Scapin[a]*

[a]Department of Medicinal Chemistry, Merck and Co., Rahway, NJ 07065, USA, and [b]Department of Metabolic Disorders, Merck and Co., Rahway, NJ 07065, USA

Correspondence e-mail: giovanna_scapin@merck.com

Received 6 October 2003
Accepted 31 October 2003

The catalytic domain of human phosphodiesterase 3B has been cloned, expressed in *Escherichia coli* and purified in the presence of the PDE3 inhibitors IBMX (3-isobutylmethylxanthine) or MERCK1 by affinity chromatography. Initial screening of crystallization conditions for these complexes in the hanging-drop vapor-diffusion mode resulted in three different crystal forms, all characterized by quite large unit-cell parameters, elevated solvent content and poor diffraction quality. Subsequent optimization of these conditions led to crystals that diffract to 2.4 Å and belong to space group *C*2, with unit-cell parameters $a = 146.7$, $b = 121.5$, $c = 126.3$ Å, $\beta = 100.6^\circ$. Rotation-function analysis indicates that the asymmetric unit contains four copies of the monomeric enzyme, corresponding to a solvent content of 64%. To solve the structure of the PDE3B catalytic domain, molecular replacement as well as multiple isomorphous replacement methods are currently being utilized.

1. Introduction

Phosphodiesterases (PDEs; EC 3.1.4.17) are a large family of enzymes catalyzing the hydrolysis of the 3′—5′ phosphodiester bond of cyclic nucleotides (cAMP and cGMP) and therefore providing a major pathway for modulating cyclic nucleotide signaling (Beavo, 1995). Changes in the intracellular concentration of cyclic nucleotide mediate the action of numerous hormones and neurotransmitter signals important for cell growth, differentiation, survival and inflammation (Francis *et al.*, 2001). At least 11 families of PDEs with varying selectivities for cAMP or cGMP have been identified in mammalian tissues. Within these families, multiple isoforms are expressed either as products of different genes or as products of the same gene through alternative splicing. The PDE3 subfamily consists of two closely related subtypes, PDE3A and PDE3B. While PDE3A is mostly expressed in cardiac tissue, platelets and vascular smooth muscle cells, PDE3B is prevalently expressed in hepatocytes and adipose tissue (Reinhardt *et al.*, 1995). PDE3B plays an important role in the stimulatory action of cAMP on pancreatic β-cell exocytosis and the release of insulin (Harndahl *et al.*, 2002). Cyclic AMP potentiates glucose-stimulated insulin release and mediates the stimulatory effects of hormones such as glucagon-like peptide 1 (GLP-1) on pancreatic β-cells. PDE3 inhibitors have been shown to increase lipolysis in adipocytes and a specific inhibitor could be used to increase metabolic rates as a potential treatment for obesity (Elks & Manganiello, 1984; Synder, 1999). Although PDE3B is a membrane-associated protein, the catalytic domain can be independently expressed as soluble enzyme and has been shown to retain catalytic activity (He *et al.*, 1998; Shakur *et al.*, 2000; Chung *et al.*, 2003; Varnerin *et al.*, 2004). The only available crystal structures to date for a member of the phosphodiesterase family are those of PDE 4B2B (Xu *et al.*, 2000), PDE4D (Lee *et al.*, 2002) and PDE5A (Sung *et al.*, 2003). Given the fact that different PDEs can be targeted for different therapeutical reasons, it is necessary to understand the reasons for the specificity of these enzymes and address the issue of selective inhibitors. In order to facilitate the development of compounds specifically targeting the 3B isoform, we undertook structural studies of the PDE3B catalytic domain. We report here the crystallization and preliminary X-ray diffraction studies of the enzyme in complex with two chemically different inhibitors, a first important step towards the structure elucidation of PDE3B.

2. Protein expression and purification

Recombinant human PDE3B was expressed and purified as described elsewhere (Varnerin *et al.*, 2004). The last step of the purification involves an affinity column from which the enzyme was eluted with the ligand of interest (IBMX or MERCK1; Edmondson *et al.*, 2003; Fig. 1). Six different constructs truncated at the N-terminus between residues 636 and 665 and one additional construct extended at the C-terminus were initially made for biochemical characterization and crystallization studies (Table 1; Varnerin *et al.*, 2004). Based on

preliminary crystallization, the 654–1073 construct was selected for exhaustive crystallization screening. The aggregation state of the protein was routinely checked by dynamic light-scattering (DLS) analysis. A critical aspect of successful crystallization trials was the buffer in which the protein was stored. The optimal protein buffer was identified by analyzing the effects of several components on the aggregation state of the enzyme using DLS analysis. Buffer *A* [10 m*M* HEPES pH 7.5, 10 m*M* NaCl, 8 m*M* $MgCl_2$, 0.25 m*M* tris(2-carboxyethyl)-phosphine hydrochloride (TCEP), 0.5% methanol, 0.01% *n*-octylglucoside] allowed the protein to remain monodisperse over several days at 277 K and was selected as the buffer of choice.

3. Crystallization

Initial crystallization conditions were screened with the sparse-matrix approach as described by Jancarik & Kim (1991). Crystallization trials were set up in a Q plate II (Hampton Research) using the hanging-drop vapor-diffusion method at room temperature with Hampton Research Crystal Screen Kits I and II. Each hanging droplet on a siliconized cover slip consisted of 1 µl of protein solution (IBMX complex; 20 mg ml^{-1} in buffer *A*) and 1 µl of one of the precipitating solutions. The reservoir contained 0.5 ml of the same precipitant. Optimization of the most promising condition (30% PEG MME 5K, 0.1 *M* MES pH 6.5, 0.2 *M* ammonium sulfate) at room temperature produced relatively thin needles (crystal form I). The crystallization conditions were further optimized by varying precipitant concentration, pH and temperature. A dramatic improvement in the size of the crystals was observed by replacing the ammonium sulfate with magnesium sulfate and lowering the PEG MME concentration to 10–12%. The use of sitting drops (3 µl protein plus 3 µl precipitant) and incubation at 277 K also played an important role in obtaining larger crystals (crystal form II; Fig. 2*a*). Interestingly, under the same conditions, the PDE3B–MERCK1 complex produced morphologically different crystals (crystal form III; Fig. 2*b*). Crystals of both complexes were difficult to vitrify upon flash-cooling though and diffracted relatively poorly. In order to further improve the quality of the crystals, several seeding and/or detergent-screening experiments were performed. The best crystals (large diamond-shaped crystal form IV; Fig. 2*c*) were obtained for the PDE3B–MERCK1 complex in the presence of detergent (1.1 m*M* nonanoyl-*H*-hydroxyethylglucamide, HEGA-9) in the well. These crystals grew to maximum dimensions of 0.3 × 0.3 × 0.1 mm.

Table 1
Constructs used in the preliminary crystallographic analysis of PDE3B.

Construct	Ligand	Preliminary crystallization results
636–1073	TBMX	Thin needles
654–1073	IBMX	Needles/rods
654–1073	MERCK1	Needles/rods
654–1086	IBMX	No leads
658–1073	IBMX	Thin needles
660–1073	IBMX	Small crystals
661–1073	IBMX	Square crystals
661–1073	MERCK1	Square crystals
665–1073	IBMX	Small crystals

4. Preliminary X-ray analysis

All diffraction data were collected under cryogenic conditions (100 K) in the facilities of the Industrial Macromolecular Crystallography Association Collaborative Access Team (IMCA-CAT) at the Advanced Photon Source (Argonne National Laboratory, Argonne, IL, USA). Before freezing, crystals of form I were immersed for several seconds in reservoir solution supplemented with 15% glycerol as a cryoprotectant. For crystal forms II, III and IV, cryoprotection was performed by immersing the crystals for a few seconds in three solutions containing 6, 12 and 25% ethylene glycol. All crystals were flash-cooled in a cold nitrogen stream. Crystal form I was characterized as monoclinic, space group $P2_1$, with unit-cell parameters a = 168.2, b = 101.5, c = 185.3 Å, β = 100.7°. These crystals were generally characterized by a very high mosaicity (greater than 2°), high anisotropy in the diffraction pattern and a relatively low diffraction limit (3.9 Å) and no complete data set was collected. Crystal form II was characterized as monoclinic *C*2, with a = 275.1, b = 147.1, c = 253.6 Å, β = 109.8°. A

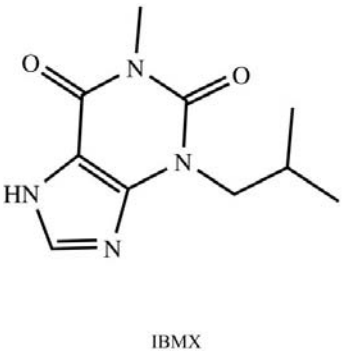

IBMX

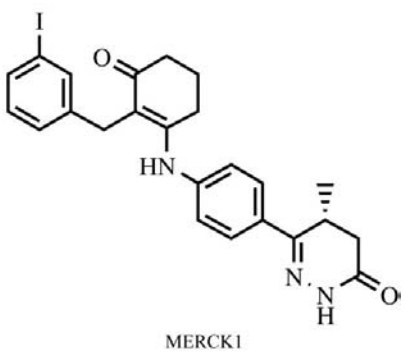

MERCK1

Figure 1
Chemical structure for the two compounds used in the crystallization trials of the catalytic domain of PDE3B.

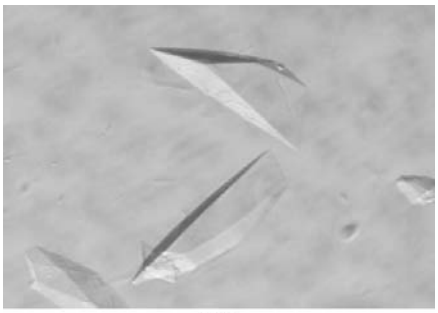

(*a*)

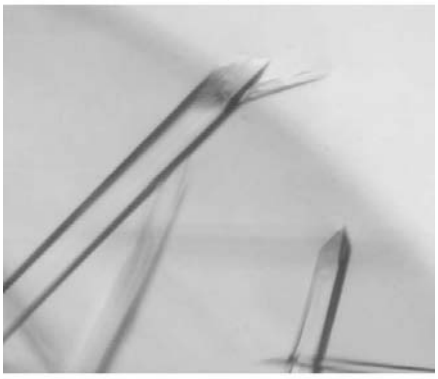

(*b*)

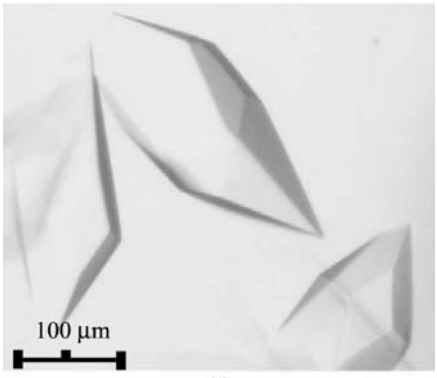

(*c*)

Figure 2
Crystals of (*a*) PDE3B in complex with IBMX, (*b*) PDE3B in complex with MERCK1 and (*c*) PDE3B in complex with MERCK1 in the presence of HEGA-9.

Table 2
X-ray data-measurement statistics.

Values in parentheses are for the highest resolution shell (3.0–2.9 Å for form II, 3.5–3.3 Å for form III and 2.5–2.4 Å for form IV).

	Form II	Form III	Form IV
Ligand	IBMX	MERCK1	MERCK1
Space group	*C*2	*C*2	*C*2
Unit-cell parameters			
a (Å)	275.1	227.3	146.8
b (Å)	147.1	106.6	121.5
c (Å)	253.5	186.4	126.3
β (°)	109.8	133.3	100.6
Resolution range (Å)	50.0–2.9	40.0–3.3	30.0–2.4
Observed reflections	1121505	177487	461794
Unique reflections	203261	48948	85707
Completeness (%)	96.8 (82.7)	99.9 (99.9)	99.8 (99.7)
$R_{\rm merge}$ (%)	11.1 (43.4)	16.3 (41.1)	6.7 (32.0)
$\langle I/\sigma(I)\rangle$	4.8 (1.0)	4.4 (1.8)	9.4 (2.1)

96.8% complete data set to 2.9 Å was collected on a MAR 165 CCD at beamline IMCA-17-BM. The data were indexed, integrated and scaled using *HKL*2000 (Otwinowski & Minor, 1997). Table 2 summarizes the data-collection statistics. The molecular weight of the enzyme is approximately 48 kDa and the volume of the asymmetric unit (AU) is approximately 2 403 700 Å; the distribution range of the volume-to-mass ratio ($V_{\rm M}$) values (Matthews, 1968; Kantardjieff & Rupp, 2003) indicates that the form II crystals may contain between ten and 24 molecules per AU. The ambiguity was solved by calculating a self-rotation map (*MOLREP*; Vagin & Teplyakov, 1997), which clearly showed a 622 symmetry and suggested that the AU probably contains 12 copies of the monomeric enzyme, corresponding to a $V_{\rm M}$ of 4.15 Å^3 Da^{-1} and a solvent content of approximately 70%. The possibility of having 24 copies of the protein in the AU (corresponding to a $V_{\rm M}$ of 2.07 Å^3 Da^{-1} and a solvent content of ∼41%), although not completely discarded, was considered quite unlikely given the low-resolution limits that characterize this crystal form. Complete data sets for crystal forms III and IV were collected on a ADSC Q210 CCD at beamline IMCA-17-ID and indexed, integrated and scaled in *HKL*2000. Crystal form III is monoclinic, space group *C*2, with a = 227.3, b = 106.6, c = 186.4 Å, β = 133.3° and $d_{\rm min}$ = 3.3 Å. The self-rotation map suggests the presence of five copies of the enzyme, corresponding to a crystal packing density of 3.4 Å^3 Da^{-1} and a solvent content of approximately 64%. Crystal form IV is also monoclinic, space group *C*2, with a = 146.7, b = 121.5, c = 126.3 Å, β = 100.6° and $d_{\rm min}$ = 2.4 Å. Assuming four molecules per AU, the $V_{\rm M}$ value is 2.8 Å^3 Da^{-1} and the solvent content is 56%. The self-rotation map showed the presence of two twofold axes separated by ∼60°, suggesting the presence of four monomers. It has been reported that all mammalian PDEs appear to exist as dimers of catalytic subunits (Beavo, 1995). In addition, the PDE3B catalytic domain was shown to be in a trimeric aggregation state in size-exclusion chromatography (Varnerin *et al.*, 2004) and detergent was necessary to improve both the homogeneity of the protein sample and the quality of the crystals in the present work. Thus, it appears that under crystallization conditions the catalytic domain of PDE3B tends to oligomerize. It remains to be determined if this aggregation state represents the true biological assembly.

The structure determination of the catalytic domain of PDE3B by the molecular-replacement and multiple isomorphous replacement (MIR) methods on form II, III and IV crystals using the three-dimensional structure of PDE4B2B as a search model is now in progress.

We thank the staff of the IMCA beamline for excellent technical support during data collection. Use of the IMCA-CAT beamlines at the Advanced Photon Source was supported by the companies of the Industrial Macromolecular Crystallography Association through a contract with Illinois Institute of Technology (IIT), executed through IIT's Center for Synchrotron Radiation Research and Instrumentation. Use of the Advanced Photon Source was supported by the US Department of Energy, Basic Energy Sciences, Office of Science under Contract No. W-31-109-Eng-38.

References

Beavo, J. A. (1995). *Physiol. Rev.* **75**, 725–743.
Chung, C., Varnerin, J., Morin, N. R., MacNeil, D. J., Singh, S. B., Patel, S., Scapin, G., Van der Ploeg, L. & Tota, M. R. (2003). *Biochem. Biophys. Res. Commun.* **307**, 1045–1050.
Edmondson, S. D., Mastracchio, A., He, J., Chung, C. C., Forrest, M. J., Hofsess, S., Macyntire, E., Metzger, J., O'Connor, N., Patel, K., Tong, X., Tota, M. R., Van Der Ploeg, L. H. T., Varnerin, J. P., Fisher, M. H., Wyvratt, M. J., Weber, A. E. & Parmee, E. R. (2003). *Bioorg. Med. Chem. Lett.* **13**, 3983–3987.
Elks, M. L. & Manganiello, V. C. (1984). *Endocrinology*, **115**, 1262–1268.
Francis, S. H., Turko, I. V. & Corbin, J. D. (2001). *Prog. Nucleic Acid Res. Mol. Biol.* **65**, 1–52.
Harndahl, L., Jing, X.-J., Iversson, R., Degerman, E., Ahren, B., Manganiello, V. C., Renstrom, E. & Stenson Holst, L. (2002). *J. Biol. Chem.* **277**, 37446–37455.
He, R., Komas, N., Ekholm, D., Murata, T., Taira, M., Hockman, S., Dergerman, E. & Manganiello, V. C. (1998). *Cell Biochem. Biophys.* **29**, 89–111.
Jancarik, J. & Kim, S.-H. (1991). *J. Appl. Cryst.* **24**, 409–411.
Kantardjieff, K. A. & Rupp, B. (2003). *Protein Sci.* **12**, 1865–1871.
Lee, M. E., Markowitz, J., Lee, J. O. & Lee, H. (2002). *FEBS Lett.* **530**, 53–58.
Matthews, B. W. (1968). *J. Mol. Biol.* **33**, 491–497.
Otwinowski, Z. & Minor, W. (1997). *Methods Enzymol.* **276**, 307–326.
Reinhardt, R. R., Chin, E., Zhou, J., Taira, M., Murata, T., Manganiello, V. C. & Bondy, C. A. (1995). *J. Clin. Invest.* **95**, 1528–1538.
Shakur, Y., Takeda, K., Kenan, Y., Yu, Z. X., Rena, G., Brandt, D., Houslay, M. D., Degerman, E., Ferrans, V. J. & Manganiello, V. C. (2000). *J. Biol. Chem.* **275**, 38749–38761.
Sung, B.-J., Hwang, K. Y., Jeon, Y. H., Lee, J. I., Heo, Y.-S., Kim, J. H., Moon, J., Yoon, J. M., Hyun, Y.-L., Kim, E., Eum, S. J., Park, S.-Y., Lee, J.-O., Lee, T. G., Ro, S. & Cho, J. M. (2003). *Nature (London)*, **425**, 98–101.
Synder, P. B. (1999). *Emerg. Ther. Targets*, **3**, 587–599.
Vagin, A. & Teplyakov, A. (1997). *J. Appl. Cryst.* **30**, 1022–1025.
Varnerin, J. P., Chung, C. C., Patel, S. B., Scapin, G., Parmee, E. R., Morin, N., MacNeil, D., Cully, D. F., Van der Ploeg, L. & Tota, M. R. (2004). Submitted.
Xu, R. X., Hassell, A. M., Vanderwall, D., Lambert, M. H., Holmes, W. D., Luther, M. A., Rocque, W. J., Milburn, M. V., Zhao, Y., Ke, H. & Nolte, R. T. (2000). *Science*, **288**, 1822–1825.